Polymer 51 (2010) 730–737

Contents lists available at ScienceDirect

Polymer

journal homepage: www.elsevier.com/locate/polymer

Morphology, rheology and crystallization behavior of polylactide composites prepared through addition of five-armed star polylactide grafted multiwalled carbon nanotubes

Zhaohua Xu [a,b], Yanhua Niu [a], Liang Yang [a,b], Wenyuan Xie [a,b], Heng Li [c], Zhihua Gan [a], Zhigang Wang [a,*]

[a] CAS Key Laboratory of Engineering Plastics, Beijing National Laboratory for Molecular Sciences, Institute of Chemistry, Chinese Academy of Sciences, Beijing 100190, PR China
[b] Graduate School, Chinese Academy of Sciences, Beijing 100049, PR China
[c] Department of Physics, Beihang University, Beijing 100191, PR China

ARTICLE INFO

Article history:
Received 26 October 2009
Received in revised form
14 December 2009
Accepted 14 December 2009
Available online 29 December 2009

Keywords:
Carbon nanotubes
Polylactide
Composites

ABSTRACT

Functionalized multiwalled carbon nanotubes (F-MWNTs) were prepared by covalent grafting of five-armed star polylactide (fa-PLA), and were characterized by thermogravimetric analysis (TGA), nuclear magnetic resonance (NMR) spectroscopy and Raman spectroscopy. A series of polylactide (PLA)/F-MWNTs composites was prepared via coagulation method. Several techniques were applied to investigate the effects of F-MWNTs on the morphology, melt rheology, and crystallization and melting behaviors of the PLA composites. The optical microscope (OM), field-emission scanning electron microscope (FE-SEM) and transmission electron microscopy (TEM) observations demonstrated that, in comparison with the case of PLA filled with pristine MWNTs, F-MWNTs case showed improved dispersion and interfacial adhesion. Oscillatory frequency sweep measurements showed that addition of about 2.0 wt% F-MWNTs led to a solidlike response where a percolated network structure formed, and the composites exhibited remarkable improvement of rheological properties in the melt state as compared with that of neat PLA. DSC measurements showed that F-MWNTs acted as a nucleating agent to enhance crystallization when below the percolation concentration, while also acted as a hindrance to retard crystallization above the percolation concentration. The double melting peaks on the DSC curves were attributed to melting of the crystals formed in the cold crystallization stage and the melting-recrystallization–remelting (mrr) event during heating, respectively.

1. Introduction

Polylactide (PLA), as a biodegradable polymer, has attracted great interest due to its good mechanical properties, thermal plasticity, and facile fabrication, thus being a promising polymer for various end-use applications. However, some of the weaknesses such as brittleness, low heat distortion temperature, poor gas barrier, etc. restrict its use in a wide-range of applications [1,2]. Increasing realization of various intrinsic properties of PLA, coupled with knowledge of how such properties can be improved to achieve compatibility with thermoplastics processing, manufacturing, and end-use requirements, has arisen academic and commercial interests.

On the other hand, the preparation of composites with carbon nanotubes (CNTs) has been proven an effective way to modify polymers [3]. CNTs, since their discovery by Iijima in 1991, have drawn increasing attention owing to their unique structures and physical properties [4]. However, as a kind of filler for polymer composites, CNTs face the challenge of achieving appropriate dispersion in polymer. Covalent functionalization with polymers can be used to disperse carbon nanotubes in various polymers, as this ensures interactions between the two components and precludes phase segregation, which includes the "grafting from" and "grafting to" approaches [5]. The "grafting from" approach relies on the growth of polymers from the CNTs surface by *in situ* polymerization of monomers promoted by initiators [6,7]. However, multiple synthetic steps must be carried out, and polymer characterization is only possible if the grafted chains can be cleaved from the nanotubes surface. The "graft to" approach comprises amidation or esterification reactions between amine or hydroxyl groups of functionalized polymers and the carboxylic groups created on the CNTs surface by oxidation with sulfuric acid, nitric acid or mixture thereof. Compared with the "grafting from" method, it suffers from low theoretical polymer loadings due to

* Corresponding author. Tel./fax: +86 10 62558172.
E-mail address: zgwang@iccas.ac.cn (Z. Wang).

0032-3861/$ – see front matter © 2009 Elsevier Ltd. All rights reserved.
doi:10.1016/j.polymer.2009.12.017

steric repulsion between grafted and reacting polymer chains but allows for characterization of polymer chains prior to grafting and avoids the structure uncertainty of the grafted polymers. By this method, linear polymers such as poly(m-aminobenzene sulfonic acid) (PABS) and ethylenediamine (EN) [8], polyethylene (PE) and chitosan [9] etc., are successfully bonded onto CNTs. Chen et al. obtained PLA-functionalized MWNTs by using the "grafting to" esterification reaction [10,11]. Yang et al. prepared six-armed star PLA-functionalized MWNTs by introducing triphenylene core through a non-covalent method [12]. However, to our knowledge, few reports focus on grafting the branched PLA onto MWNTs by covalent method. From the interaction viewpoint, it is expected that the branched PLA-functionalized MWNTs and their composites with PLA might present good dispersion and largely enhanced physical properties.

It is well known that rheological properties and crystallization behavior are very important for polymer processing and application. It is also necessary to correlate rheological properties and crystallization behavior with the composite structures [13]. Wu et al. used rheological method to examine the dispersion of different functionalized MWNTs in PLA and found that the carboxylic MWNTs present better dispersion in PLA than the hydroxyl MWNTs, which led to the non-terminal low frequency behavior due to the readily formed network structure [14]. Song investigated the rheological behaviors of PEO/CNTs composites with different surface treatments to CNTs and found that the acid-treated CNTs composites exhibited higher complex viscosity [15]. It was also reported that the so-called 'percolation threshold concentration' was strongly dependent on the measurement temperature [16]. Besides improved processing of polymer composites, CNTs also affected polymer crystallization through heterogeneous nucleation effect. Zhao's study revealed that the overall crystallization rate of PLA increased with increasing MWNTs content [3]. However, for some polar polymers such as polyamide 6 (PA6) and polyethylene oxide (PEO) the crystallization rates of polymers in the composites unexpectedly decreased in contrast to neat polymers [17,18]. Shieh et al. studied the crystallization and melting behaviors of PLA-functionalized CNTs/PLA composites and found that CNTs significantly enhanced the nonisothermal crystallization. Furthermore, the appeared double melting peaks could be attributed to polymer recrystallization and melting, respectively [19]. Obviously, there seem no consistent results and explanations to how CNTs affect the crystallization behaviors of composites. In our previous investigation, the effects of percolated CNTs network on the isothermal crystallization behavior of iPP were thoroughly discussed, in which the results indicated that below the percolation concentration, CNTs could largely accelerate the crystallization rates of iPP, while beyond that concentration, CNTs network might restrict the mobility and diffusion of iPP chains to crystal growth fronts and finally the crystallization rate of iPP did not change obviously [20]. In this work, similar effects of the percolated network on the crystallization behavior in PLA/F-MWNTs composites were found, which strongly supported the restriction effect of the CNTs network on polymer chains diffusion.

We herein first focused on the covalent bonding of five-armed star polylactide (fa-PLA) molecules to MWNTs by the "grafting to" method. The covalent bonding of fa-PLA to MWNTs (F-MWNTs) was examined by using TGA, ^{1}H NMR and Raman spectroscopy. The PLA/F-MWNTs composites were prepared by coagulation method and the dispersion of F-MWNTs was evaluated by optical microscope (OM), field-emission scanning electron microscope (FE-SEM) and transmission electron microscopy (TEM). On the basis of good dispersion of CNTs in composites, we further investigated the effects of F-MWNTs content on the melt rheological properties and crystallization behavior of PLA/F-MWNTs composites.

2. Experimental section

2.1. Materials

A commercial polylactide (PLA, trade name 4032D, from NatureWorks Co. Ltd., USA) was used in this work. It had weight-averaged molecular mass (M_w) and polydispersity (M_w/M_n) of ca. 160 000 g/mol and 1.67, respectively, measured by the Waters 2414 GPC. The multiwalled carbon nanotubes (MWNTs, purity > 95%, made by chemical vapor deposition method) with diameter of 10–20 nm, length of 0.5–2 μm, and aspect ratio of 25–200 were supplied by ChengDu Organic Chemistry Co. Ltd, Chinese Academy of Sciences. Lactide (LA) monomer was kindly provided by Changchun Institute of Applied Chemistry, Chinese Academy of Sciences and was purified by recrystallization in acetic ester. Stannous octoate ($SnOct_2$) (from Aldrich Chemical) was dissolved in dehydrated toluene prior to use. Toluene was purified by distillation in the presence of metallic sodium and benzophenone. Erythritol (AR grade, from Acros Organics) was fully dried at 50 °C in vacuum. The M_w and polydispersity (M_w/M_n) of the obtained fa-PLA were 96 000 g/mol and 1.19, respectively. Other reagents, thionyl chloride ($SOCl_2$), *N*, *N*-dimethylformamide (DMF), methylene chloride ($CHCl_2$) and chloroform ($CHCl_3$), were purchased from the Beijing Chemical Reagents Company and were dried before use.

2.2. Preparation of fa-PLA, F-MWNTs and PLA/F-MWNTs composites

In this work, five-armed star PLA as well as linear PLA were synthesized *via* ring-opening polymerization of L-lactide monomer with erythritol as initiator and $Sn(Oct)_2$ as catalyst. The polymerization procedure for five-armed star PLA was similar to the one for star-shaped PCL described in our previous and Korhonen's work [21]. Fig. 1(a) shows the synthetic pathway for the five-armed star PLA. The typical polymerization procedure is described as follows: a dried glass reaction tube was degassed and purged with argon three times. Then the predetermined amounts of LA monomer, toluene, initiator, and catalyst were added in sequence into the tube. After the tube was sealed, it was immersed into an oil bath set at 110 °C for 48 h. The reaction mixture was cooled and dissolved in methylene chloride, and then was precipitated in excess methanol. After dissolving in methylene chloride and precipitating in methanol three times, the obtained products were dried in vacuum under ambient temperature for at least 48 h before further characterization.

F-MWNTs were prepared *via* the acid-thionyl chloride method as shown in Fig. 1(b) according to the method of Chen et al. [10]. The pristine MWNTs (P-MWNTs) were mixed with sulfuric (98%) and nitric (68%) acids (3:1 in volume) and treated in ultrasonic bath for 1 h, and then refluxed at 60 °C for 4 h. Excess acid was washed thoroughly with deionized water until the pH value was about 7.0. The acid-treated MWNTs (A-MWNTs) were dried in vacuum at 60 °C overnight and then ground to powder in an agate mortar. The mixture of A-MWNTs, thionyl chloride ($SOCl_2$), and *N*, *N*-dimethylformamide (DMF) (a typical ratio of A-MWNTs/$SOCl_2$/DMF is 1 g/60 ml/2 ml) was treated in an ultrasonic bath for 2 h and then refluxed at 70 °C for 24 h. Then, $SOCl_2$ was removed by distillation and the remained black solid was reacted with excess fa-PLA in N_2 atmosphere at 60 °C for 48 h; afterwards, the black solid was washed with anhydrous $CHCl_3$ about five times, and then placed in a Soxhlet extractor with anhydrous $CHCl_3$ of 200 ml employed as extracting solvent to remove unattached fa-PLA for 24 h [7,22]. Finally, the obtained fa-PLA-grafted MWNTs (F-MWNTs) were placed in vacuum at 60 °C for 48 h to remove solvents before further use.

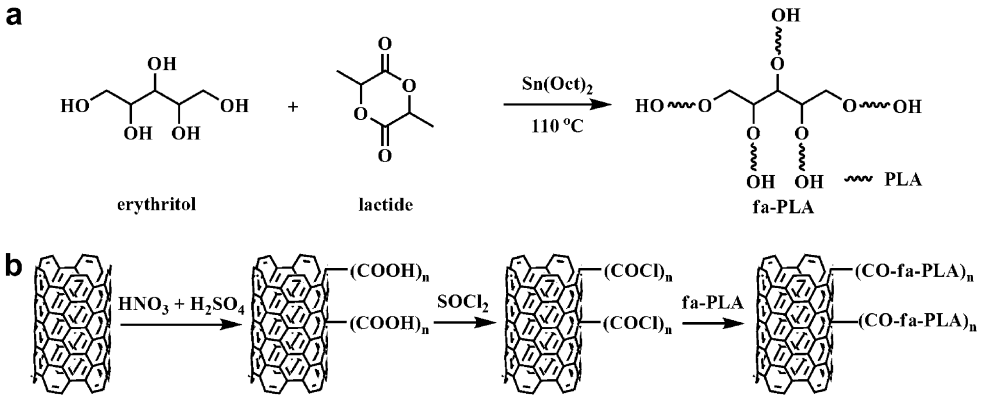

Fig. 1. The covalent route for preparation of (a) five-armed star PLA (fa-PLA) and (b) fa-PLA-functionalized MWNTs (F-MWNTs).

The coagulation method was used to prepare the PLA/F-MWNTs composites. At first, PLA was dissolved in $CHCl_3$ at room temperature and F-MWNTs were dispersed in $CHCl_3$ in ultrasonic bath (200 W and 45 kHz) for 1 h. Then, the F-MWNTs/$CHCl_3$ suspension was added into PLA/$CHCl_3$ solution with vigorous stir for 1.5 h. The suspension was poured into a large amount of cold CH_3OH afterwards. After filtration and drying in vacuum at 60 °C for 48 h, the PLA/F-MWNTs composite was obtained. In this work, the F-MWNTs mass concentration was designed as 0, 0.5, 1.0, 2.0, 4.0, 6.0 and 8.0 wt%, respectively.

2.3. Molecular structure characterization of F-MWNTs

Thermogravimetric analyses (TGA) of F-MWNTs and other MWNTs were performed on a TGA-Pyris 1 (Perkin–Elmer Instruments, USA) at a heating rate of 20 °C/min from 50 to 750 °C in N_2 atmosphere. ^{1}H NMR spectra of MWNTs were recorded on a Bruker AV 400 spectrometer (Bruker Corporation, Germany) at 400 MHz with tetramethylsilane (TMS) as internal reference standard and deuterated chloroform ($CDCl_3$) as solvent. Raman spectra of MWNTs were recorded on a Renishaw-2000 Raman spectrometer (Wotton-under-Edge, Gloucestershire, UK) at a resolution of 2 cm^{-1} by using the 514.5 nm line of an Ar ion laser as the excitation source.

2.4. Dispersion evaluation of F-MWNTs in the composites

Optical microscope (OM, Olympus BX51, Japan) equipped with a CCD camera (HV1301UC, Beijing Daheng, China) was used to examine the dispersion state of F-MWNTs in the PLA composites. The PLA composites were melt-compressed into films with thickness of about 40 μm for this observation. The field-emission scanning electron microscope (FE-SEM, Hitachi S-530, Japan) was used to observe the morphologies of the fractured surface of the PLA composites. The PLA composites were quenched into liquid nitrogen and then fractured. The fractured surfaces were sputtered with platinum before observation. Ultrathin samples for transmission electron microscopy (JEOL JEM-2200FS, Japan) observations were cut from the PLA composites under cryogenic conditions (−80 °C) using a Leica EM FC6 ultramicrotome.

2.5. Rheological measurements on PLA/F-MWNTs composites

To measure the rheological properties of the PLA/F-MWNTs composites, a stress-controlled rheometer (TA Series AR2000, TA Instruments, USA) was employed using parallel-plate geometry (diameter of 25 mm) under nitrogen atmosphere. Before rheological measurements, the dried PLA/F-MWNTs composites were pressed at 180 °C in vacuum into disks with a thickness of 1 mm and diameter of 25 mm in stainless steel dies. The samples were further dried in vacuum at 60 °C for 6 h. Oscillatory frequency sweeps ranging from 0.1 to 500 rad/s with a fixed strain of 1.0% (falling in the linear viscoelasticity region) were performed at 180 °C for the seven PLA/F-MWNTs composite samples. After sample loading, approximate 5 min equilibrium time was applied prior to each frequency sweep run.

2.6. Crystallization and melting behaviors of PLA/F-MWNTs composites

Crystallization and melting behaviors of PLA/F-MWNTs composites were studied by using a TA Q200 differential scanning calorimeter (DSC). Samples with ca. 5 mg mass were firstly heated to 190 °C and held for 3 min to erase previous thermal history (the first heating scan), and then cooled to 10 °C at a cooling rate of 10 °C/min (the first cooling scan). The subsequent heating scan from 10 °C to 190 °C at 10 °C/min (the second heating scan) was recorded, from which the glass transition temperature, cold crystallization temperature and melting point of the sample were obtained. The effect of heating rate (heating rates of 2, 5, 10, 20, 30 and 40 °C/min) was examined for the PLA/F-MWNTs composite with F-MWNTs mass concentration of 0.5%.

3. Results and discussion

3.1. Characterization of F-MWNTs by TGA, NMR and Raman

It is well known that the defunctionalization of carbon nanotubes can be realized by thermal decomposition [11,23]. Fig. 2 shows the TGA curves of pristine MWNTs (P-MWNTs), MWNTs-COOH (A-MWNTs), F-MWNTs and neat fa-PLA in nitrogen atmosphere. The obvious differences among the four samples can be seen. Neat fa-PLA decomposes nearly 98.7 wt% before the temperature reaches 400 °C. MWNTs hardly decompose below 750 °C and about 99.0% mass remains at 750 °C. However, the mass losses of 5.6% for A-MWNTs and 22.6% for F-MWNTs at 750 °C are observed. The difference in mass loss at 750 °C between A-MWNTs and F-MWNTs indicates that the fa-PLA grafting amount is about 17.0 wt%, which is slightly higher than that used in the Olalde's study in which the "grafting to" method was used to graft nearly the same molecular mass linear PLA to MWNTs [11]. This can be attributed to the fact that the fa-PLA can supply more hydroxyls reacting with acyl chloride-functionalized MWNTs. Chen et al. also found that the grafting amount strongly depended on the grafted linear PLA molecular mass and there was an optimal molecular

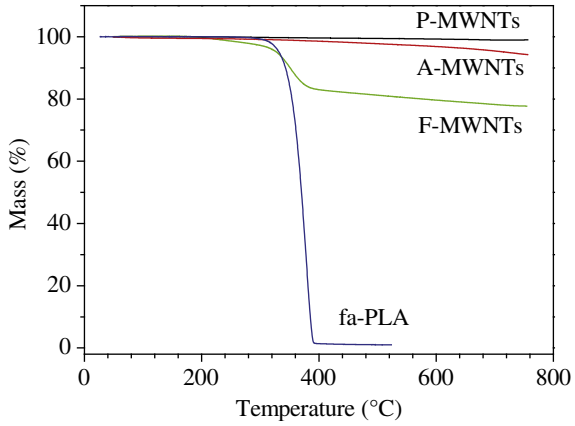

Fig. 2. TGA curves of pristine MWNTs (P-MWNTs), MWNTs-COOH (A-MWNTs), fa-PLA-grafted MWNTs (F-MWNTs) and neat fa-PLA.

mass for functionalization of MWNTs when PLA molecular mass was beyond 15 000 g/mol and the grafting amount was lower than 25 wt% [10]. In addition, different onset decomposition temperatures can also be discerned from the TGA curves. The mass loss at 180 °C for A-MWNTs is due to the decomposition of the grafted carboxylic groups. The mass loss at about 200 °C for F-MWNTs reflects debonding of the carbonyl of the grafted fa-PLA. The obvious mass loss at around 300 °C is due to decomposition of polymer backbones [23]. The different decomposition temperatures and mass losses between A-MWNTs and F-MWNTs bring out the conclusion that fa-PLA is successfully grafted on MWNTs.

The chemical structures of F-MWNTs can be confirmed by ^{1}H NMR as shown in Fig. 3. The ^{1}H NMR spectra of F-MWNTs and fa-PLA in $CDCl_3$ at 25 °C appear rather similar. The characteristic peaks of fa-PLA at $\delta = 5.17$ and 1.58 ppm are respectively ascribed to –CH and $-CH_3$ protons of PLA repeat unit, while the two peaks at $\delta =$ 4.36 ppm (see inset of Fig. 3) are attributed to $-CH_2$ protons of co-initiator erythritol and –CH proton next to the terminal hydroxyl, $-CH_2OH$ [24]. The F-MWNTs spectrum also shows nearly the same characteristic peaks at $\delta = 5.17$ and 1.58 ppm. Note that inset of Fig. 3 also shows one broad peak at $\delta = 4.36$ ppm for F-MWNTs, which is in part due to the heterogeneous nature of dispersion, in addition to the high molecular mass of grafted PLA and low mobility of carbon nanotubes [25]. Considering that unattached fa-PLA has been removed by filtration and extraction, the ^{1}H NMR result is indicative of the nanotubes functionalization with fa-PLA.

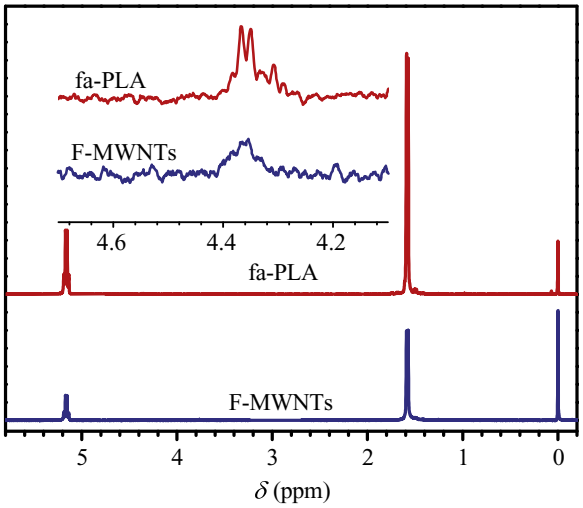

Fig. 3. ^{1}H NMR spectra of F-MWNTs and neat fa-PLA.

Raman spectroscopy was used to examine the structural modifications of the nanotube walls by different chemical species [26]. The Raman spectra in Fig. 4 show the existence of *D* band (ca.1344 cm^{-1}) and *G* band (ca.1570 cm^{-1}) for both F-MWNTs and P-MWNTs. The *D* band is assigned to the disordered graphite structure or sp^3-hybridized carbons of the nanotubes, and the *G* band to a splitting of the E_2g stretching mode of graphite which reflects the structural intensity of sp^2-hybridized carbons. The relative degree of functionalization on the nanotubes can be evaluated by the intensity ratio of *D* band and *G* band (the *D*/*G* ratio), which represents the degree of functionalization or defects on the nanotubes [11,27]. The *D*/*G* ratio increases from 1.0 for P-MWNTs to 1.2 for F-MWNTs suggesting a higher density of sp^3-hybridized carbon "defect" sites formed on the nanotube walls due to attachments of fa-PLA, which is a direct evidence of functionalization from the Raman analysis [28].

3.2. Dispersion of MWNTs in PLA

The dispersion of MWNTs in polymer is one of the most important topics for fabricating high performance polymer/MWNTs composites. A homogeneous dispersion of MWNTs and strong interfacial interactions between polymer matrix and nanotubes can effectively improve the mechanical, electrical, and thermal properties of polymer composites [29]. The dispersions of MWNTs in PLA/P-MWNTs and PLA/F-MWNTs composites were observed by optical microscope (OM) and the typical micrographs of the composites with MWNTs concentration of 1.0 wt% are shown in Fig. 5 as examples. In Fig. 5(a), numerous P-MWNTs agglomerates with sizes of approximate 10 μm or even larger in sizes can be found in the PLA matrix. On the contrary, F-MWNTs are found to be uniformly distributed at a submicrometer scale as shown in Fig. 5(b) for the PLA/F-MWNTs composite. The result indicates that F-MWNTs possess enhanced compatibility with PLA matrix through the grafted fa-PLA at F-MWNTs surface. FE-SEM micrographs of 1.0 wt% PLA/P-MWNTs and PLA/F-MWNTs composite fractured surface morphologies are shown in Fig. 5(c) and (d). It can be seen from Fig. 5(c) that P-MWNTs agglomerate in PLA matrix. However, most F-MWNTs are broken rather than pulled out from the PLA matrix (see Fig. 5(d)) indicating strong interfacial adhesion between F-MWNTs and PLA matrix for the PLA/F-MWNTs composite. The dispersion of F-MWNTs in our study is better than the case of dispersing six-armed star polylactide-functionalized MWNTs in PLA [12]. The ultrathin films of 1.0 wt% PLA/P-MWNTs and PLA/F-MWNTs composites were further observed by TEM and

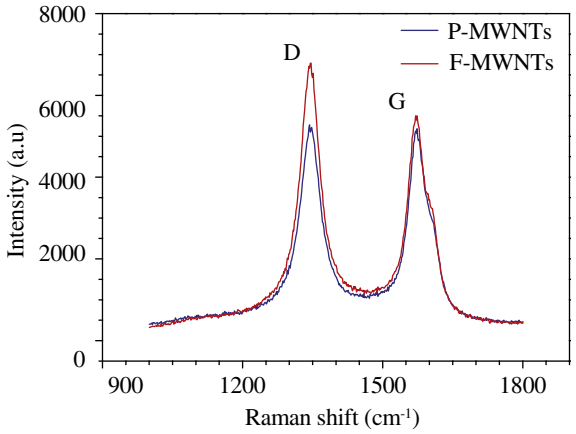

Fig. 4. Raman spectra of P-MWNTs and F-MWNTs for the excitation at 514.5 nm.

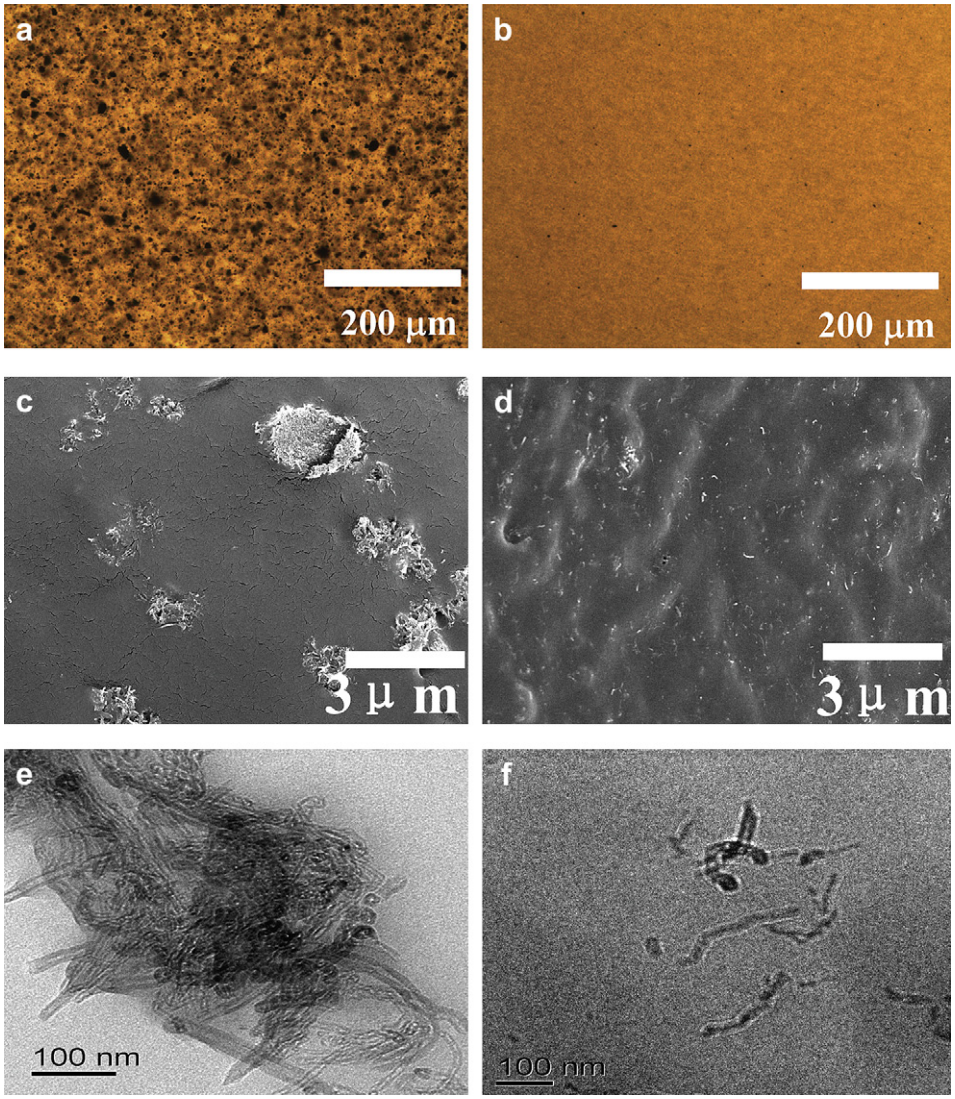

Fig. 5. Optical (a, b), FE-SEM (c, d) and TEM (e, f) micrographs for PLA/P-MWNTs composite (a, c, e) and PLA/F-MWNTs composite (b, d, f) with MWNTs concentration of 1.0 wt%.

the TEM micrographs are shown in Fig. 5(e) and (f). One can see that the individual F-MWNTs are dispersed in PLA matrix, which indicates much better dispersion for F-MWNTs than P-MWNTs. It is noticed from Fig. 5(f) that the lengths of F-MWNTs are shorter than that of P-MWNTs because our preparation process used ultrasonic, which could shorten the MWNTs. Shieh and Chen observed similar dispersion in PLA by using the "grafting to" and "grafting from" methods respectively to functionalize the CNTs [19,30]. Therefore, the covalent method can be used as an effective approach to improve CNTs dispersion. In contrast to the "grafting from" method, the "grafting to" method can produce F-MWNTs attached with well-defined polymer structures.

3.3. Influence of F-MWNTs on the melt rheological properties

To further explore the influence of F-MWNTs on the melt rheological properties of the composites, the oscillatory shear rheological measurements were carried out. Fig. 6 shows the frequency dependences of storage modulus (G'), loss modulus (G''), loss tangent ($\tan\delta$) and complex viscosity ($|\eta^*|$) for neat PLA and its composites with different F-MWNTs concentration, respectively. The moduli of the composites increase with increasing F-MWNTs concentration. At high frequencies, the qualitative behaviors of G' and G'' are essentially similar and are not affected by F-MWNTs concentration, suggesting that the F-MWNTs do not affect the PLA chains dynamics at the scales comparable to the entanglement length [31,32]. However, at low frequencies, G' and G'' increase monotonically with increasing F-MWNTs concentration. Neat PLA chains fully relax and exhibit the typical terminal behavior with the scaling law of approximate $G' \propto \omega^2$ and $G'' \propto \omega$. The values of G' and G'' for the composites containing 0.5 and 1.0 wt% F-MWNTs do not differ much from each other. With F-MWNTs concentration increasing up to 2.0 wt%, the slopes of the modulus curves of the composites change significantly, with G' nearly independent of frequency, indicating that F-MWNTs form a pseudo-solidlike network in PLA matrix. The transition from the liquidlike to solid-like viscoelastic behaviors at low frequencies demonstrates that the long-range polymer chains motion is restrained significantly by the F-MWNTs network. Meanwhile, the frequency dependence of G'' also shows the same tendency as G'.

Fig. 6(c) shows the frequency dependence of loss tangent ($\tan\delta$) for the composites with different F-MWNTs concentration. Tan δ is usually used to characterize the material viscoelasticity, which is regarded more sensitive to the relaxation changes than storage modulus (G') and loss modulus (G''). Tan δ is also dependent on F-MWNTs concentration. For the composites containing 0.5 and 1.0

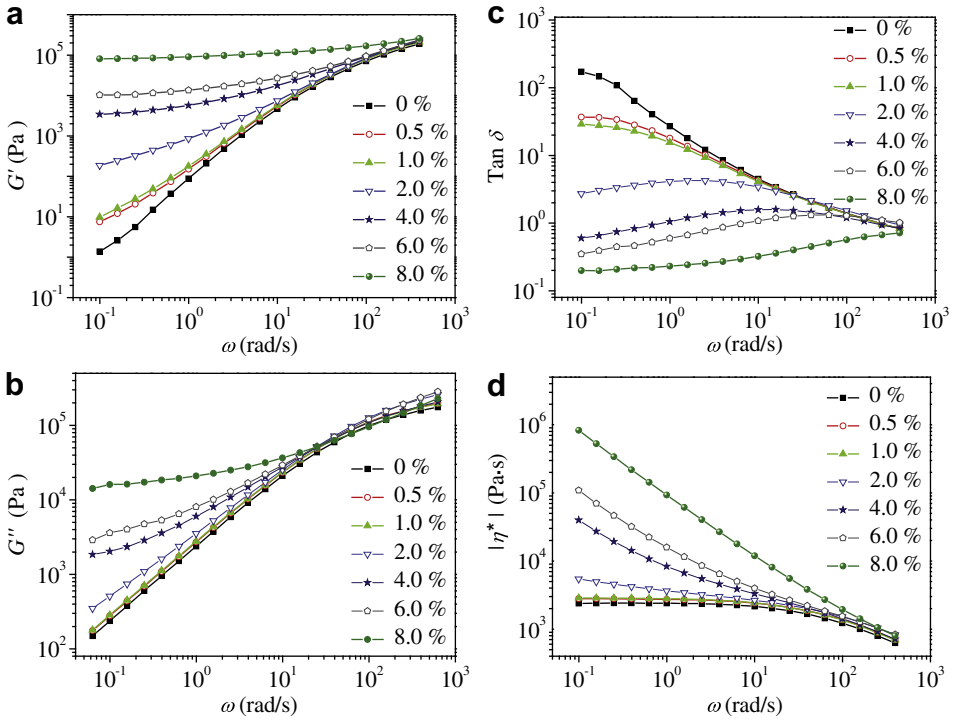

Fig. 6. Changes of (a) storage modulus (G'), (b) loss modulus (G''), (c) loss tangent (tan δ) and (d) complex viscosity ($|\eta^*|$) as functions of frequency for PLA/F-MWNTs with different F-MWNTs concentrations. The measurements were performed with a strain of 1.0 wt% at 180 °C.

wt% F-MWNTs, tan δ decreases with increasing frequency, as typical for a viscoelastic liquid. When F-MWNTs concentration reaches 2.0 wt% or above, a moderate increase of tan δ appears with increasing frequency, indicating a dominant elastic response of the sample. This means that at a certain nanotubes concentration between 1.0 and 2.0 wt%, tan δ is independent of frequency, so the F-MWNTs concentration of percolation is in between 1.0 and 2.0 wt% (more precisely to say, close to 2.0 wt%). The percolation values reported in the literature for polymer/CNTs composites vary from 0.002 to over 4.0 wt%, which are related to the CNTs dispersion state, CNTs aspect ratio and processing conditions etc. [32]. In our study the functionalization of MWNTs by fa-PLA enhances compatibility between F-MWNTs and PLA, which contributes to the low percolation concentration for the composites.

Difference in rheological response upon addition of F-MWNTs can also be noted by the changes of complex viscosity ($|\eta^*|$). It is clearly seen from Fig. 6(d) that F-MWNTs have a dramatic effect on the complex viscosity of the composites. Note that the viscosity curves for 0.5 and 1.0 wt% F-MWNTs concentration composites show similar frequency dependences as neat PLA with the Newtonian plateaus at low frequencies. However, at above 2.0 wt% F-MWNTs concentration, the viscosity curves of the composites show much steep slopes and no plateau regions are observed over the studied frequency range. The above results indicate that with increasing F-MWNTs concentration, F-MWNTs–PLA and F-MWNTs–F-MWNTs interactions are enhanced, and the composites gradually approach the percolation value, which results in an obvious increase of complex viscosity and the disappearance of the Newtonian plateau region.

3.4. Influence of F-MWNTs on crystallization and melting behaviors

Fig. 7(a) shows the DSC heating scan curves of PLA/F-MWNTs composites that are previously cooled from the melt. Both the cooling and heating scan rates are 10 °C/min. In Fig. 7(a), the shoulder peaks appearing at about 64.0 °C for all the samples correspond to the glass transition temperature (T_g) of PLA. Addition of F-MWNTs hardly affects the T_g values of the composites. It can be also seen that the neat PLA during heating exhibits an exothermic peak at 127.5 °C due to cold crystallization and a single endothermic peak due to melting. With addition of 0.5 wt% F-MWNTs, the exothermic peak appears at 114.8 °C. The peak temperature of cold crystallization (T_c) for the other composites gradually shifts to lower temperature region with increasing F-MWNTs concentration. The above results indicate that F-MWNTs enhance the cold crystallization ability of PLA, possibly through increasing the nucleation ability of PLA on F-MWNTs. On the other hand, the slight T_c shifts beyond 2.0 wt% F-MWNTs concentration are related to the percolated structures in the composites. Fillers in polymer matrix usually play dual roles, one acting as a nucleating agent to enhance crystallization when below the percolation concentration, and the other one acting as a hindrance to retard crystallization above the percolation concentration because of the formed network structure associated with high melt viscosity [20]. Our results are in accordance with Valentini and Kumar's results that the ability of nucleation is not linearly proportional to the CNT content, suggesting a saturation of the nucleation effect, particularly at high CNT contents [33,34].

It is also seen that the shape and number of the melting peaks depend on F-MWNTs concentration. For neat PLA, a single melting peak is observed. For the composite with 0.5 wt% F-MWNTs, double melting peaks with almost the same height are observed. With increasing F-MWNTs concentration, the peak height locating at lower temperature decreases while that at higher temperature increases. When the F-MWNTs concentration increases up to 6.0 wt%, the lower temperature peak starts to merge on the higher temperature peak. Generally speaking, the multiple melting behaviors are related to the presence of crystals with different crystal forms or different perfection degree or the melting–recrystallization–remelting (mrr) event

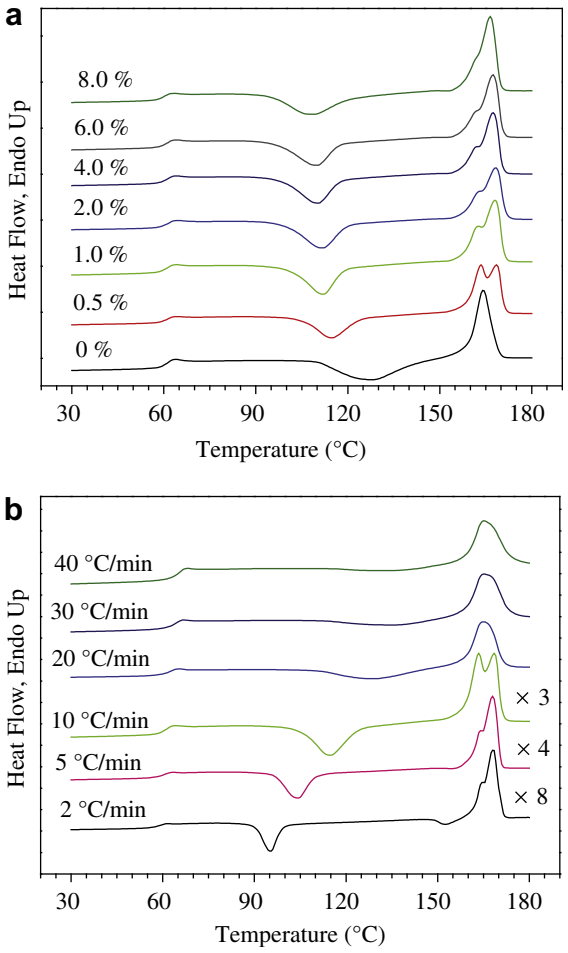

Fig. 7. DSC heating scan curves of (a) PLA/F-MWNTs composites with different F-MWNTs concentration and (b) PLA/F-MWNTs composite with 0.5 wt% F-MWNTs concentration at different heating rates. For clarity, the curves are shifted in vertical axis direction by multiplying by constants, which are remarked at the right side of the curves.

during heating [35,36]. The polymorphism behavior of PLA has been detected, which strongly relies on crystallization conditions [19]. To investigate the origin of the double melting peaks, the 0.5 wt% F-MWNTs composite sample cooled from the melt at 190 °C to 10 °C was heated up again at different heating rates. The results are shown in Fig. 7(b). It can be seen from Fig. 7(b) that the double melting peaks appear in the 2, 5 and 10 °C/min heating rate cases, but only one broad peak appears when heating rate reaches 20 °C/min or above. It can be also found that the low temperature peak height is lower than that of the higher temperature peak when the heating rate is lower than 20 °C/min, whereas the higher temperature peak disappears when the heating rate is 20 °C/min or above. The height changes of the double melting peaks with increasing heating rate indicate that the double peaks correspond to the melting of crystals formed in the cold crystallization stage and the mrr event during heating, respectively. We note here that the DSC curves during cooling of the samples do not show any exothermal peaks indicating that the crystals cannot form during cooling and the exothermal peaks during heating of the samples due to cold crystallization indicate the formation of crystals. Thus, the double melting behavior is truly due to the mechanism based on melting of the crystals formed in the cold crystallization stage during heating and followed by recrystallization and further melting processes at higher temperatures [37,38]. We also note that we have observed similar trends for neat PLA and other PLA/F-MWNTs composites as well.

4. Conclusions

In this study, a new approach is applied for preparing the covalently functionalized MWNTs (F-MWNTs) through the reaction of five-armed star polylactide with MWNTs–COCl. The results from TGA, ^{1}H NMR and Raman spectroscopy show that fa-PLA chains are successfully grafted onto the MWNTs surface and the grafting amount reaches 17 wt%. The attachments of fa-PLA chains to MWNTs enhance the compatibility between MWNTs and PLA matrix, which as a result leads to homogeneous dispersion of F-MWNTs. Rheological measurements show that addition of F-MWNTs in PLA matrix has a dramatic influence on the low frequency relaxations of PLA chains. At about 2.0 wt% F-MWNTs concentration, MWNTs form a percolated network structure. DSC measurements indicate that F-MWNTs in PLA matrix play dual roles, one acting as a nucleating agent to enhance nucleation of crystallization when below the percolation concentration, and the other one acting as a hindrance to retard crystallization above the percolation concentration. The double melting peaks during heating are observed on the DSC curves when F-MWNTs concentration is lower than 6.0 wt%, which is interpreted by the melting of crystals formed in the cold crystallization stage and the mrr event during heating, respectively.

Acknowledgment

ZG Wang acknowledges the financial support from NSFC with grant number 10590355.

References

[1] Ray SS, Bousmina M. Prog Mater Sci 2005;8:962.
[2] Sinha Ray S, Yamada K, Okamoto M, Ogami A, Ueda K. Chem Mater 2003;7:1456.
[3] Zhao YY, Qiu ZB, Yang WT. J Phys Chem B 2008;51:16461.
[4] Iijima S. Nature 1991;6348:56.
[5] Xu YY, Gao C, Kong H, Yan DY, Jin YZ, Watts PCP. Macromolecules 2004;24:8846.
[6] Zeng HL, Gao C, Yan DY. Adv Funct Mater 2006;6:812.
[7] Gao C, Jin YZ, Kong H, Whitby RLD, Acquah SFA, Chen GY, et al. J Phys Chem B 2005;24:11925.
[8] Hu H, Ni YC, Montana V, Haddon RC, Parpura V. Nano Lett 2004;3:507.
[9] Yang BX, Pramoda KP, Xu GQ, Goh SH. Adv Funct Mater 2007;17:2062.
[10] Chen GX, Kim HS, Park BH, Yoon JS. J Phys Chem B 2005;47:22237.
[11] Olalde B, Aizpurua JM, Garcia A, Bustero I, Obieta I, Jurado MJ. J Phys Chem C 2008;29:10663.
[12] Yang UP, Pan CY. Macromol Chem Phys 2008;8:783.
[13] Du FM, Scogna RC, Zhou W, Brand S, Fischer JE, Winey KI. Macromolecules 2004;37:9048.
[14] Wu DF, Wu L, Zhang M, Zhao YL. Polym Degrad Stab 2008;8:1577.
[15] Song Young S. Polym Eng Sci 2006;10:1350.
[16] Potschke P, Abdel-Goad M, Alig I, Dudkin S, Lellinger D. Polymer 2004;26:8863.
[17] Li J, Fang Z, Tong L, Gu A, Liu F. Eur Polym J 2006;12:3230.
[18] Chatterjee T, Yurekli K, Hadjiev VG, Krishnamoorti R. Adv Funct Mater 2005;11:1832.
[19] Shieh YT, Liu GL. J Polym Sci Part B Polym Phys 2007;14:1870.
[20] Xu DH, Wang ZG. Polymer 2008;1:330.
[21] Xie WY, Jiang N, Gan ZH. Macromol Biosci 2008;8:775.
[22] Buffa F, Hu H, Resasco DE. Macromolecules 2005;20:8258.
[23] Chen S, Wu G, Liu Y, Long D. Macromolecules 2006;1:330.
[24] Korhonen H, Helminen A, Seppala JV. Polymer 2001;18:7541.
[25] Qu LW, Veca LM, Lin Y, Kitaygorodskiy A, Chen BL, McCall AM, et al. Macromolecules 2005;38:10328.
[26] Abdula D, Nguyen KT, Shim M. J Phys Chem C 2007;48:17755.
[27] Sahoo NG, Jung YC, Yoo HJ, Cho JW. Macromol Chem Phys 2006;19:1773.
[28] Ma HY, Tong LF, Xu ZB, Fang ZP. Adv Funct Mater 2008;18(3):414.
[29] Tang CY, Xiang LX, Su JX, Wang K, Yang CY, Zhang Q, et al. J Phys Chem B 2008;13:3876.
[30] Chen GX, Kim HS, Park BH, Yoon JS. Macromol Chem Phys 2007;4:389.

[31] Mitchell CA, Bahr JL, Arepalli S, Tour JM, Krishnamoorti R. Macromolecules 2002;23:8825.
[32] Li J, Ma PC, Chow WS, To CK, Tang BZ, Kim JK. Adv Funct Mater 2007;16:3207.
[33] Valentini L, Biagiotti J, Kenny JM, Santucci S. J Appl Polym Sci 2003;4:708.
[34] Kumar S, Doshi H, Srinivasarao M, Park JO, Schiraldi DA. Polymer 2002;5:1701.
[35] Li J, Fang ZP, Zhu Y, Tong LF, Gu AJ, Uu F. J Appl Polym Sci 2007;6:3531.
[36] Qiu J, Xu DH, Zhao JC, Niu YH, Wang ZG. J Polym Sci Part B Polym Phys 2008;19:2100.
[37] Wu DF, Wu L, Wu LF, Xu B, Zhang YS, Zhang M. J Polym Sci Part B Polym Phys 2007;9:1100.
[38] Huang JW, Hung YC, Wen YL, Kang CC, Yeh MY. J Appl Polym Sci 2009;5: 3149.